Molecular Crystals and Liquid Crystals
Publication details, including instructions for authors and subscription information:
http://www.tandfonline.com/loi/gmcl20

Optical Properties of a Two-Photon Chromophore in a Polymeric Nanostructure

Okhil Kumar Nag [a] & Han Young Woo [a]

[a] Department of Nano Fusion Technology, Department of Cogno-Mechatronics Engineering (WCU), Pusan National University, Miryang, 627-706, Republic of Korea

Available online: 12 Jan 2012

To cite this article: Okhil Kumar Nag & Han Young Woo (2012): Optical Properties of a Two-Photon Chromophore in a Polymeric Nanostructure, Molecular Crystals and Liquid Crystals, 554:1, 65-71

To link to this article: http://dx.doi.org/10.1080/15421406.2012.633045

Mol. Cryst. Liq. Cryst., Vol. 554: pp. 65–71, 2012

ISSN: 1542-1406 print/1563-5287 online
DOI: 10.1080/15421406.2012.633045

Taylor & Francis
Taylor & Francis Group

Optical Properties of a Two-Photon Chromophore in a Polymeric Nanostructure

OKHIL KUMAR NAG AND HAN YOUNG WOO*

Department of Nano Fusion Technology, Department of Cogno-Mechatronics Engineering (WCU), Pusan National University, Miryang 627-706, Republic of Korea

*Optical properties of a cationic two-photon absorption (TPA) chromophore, 1,4-bis{4′-[*N,N*-bis(6′′-trimethylammoniumhexyl)amino]styryl}benzene tetrabromide (**C1**) upon complexation with an anionic diblock copolymer, poly[(ethylene oxide)-block-(sodium 2-acrylamido-2-methyl-1-propane sulfonate)] (**E_m-A_n**) and a cationic surfactant, cetyltrimethylammonium bromide (CTAB) have been studied. Electrostatic interaction among **C1**, cationic CTAB and anionic (**E_m-A_n**) forms a vesicular polymeric nanostructure (containing **C1** in a core), which is soluble in water. Incorporation of **C1** into the nonpolar microenvironment inside the nanostructure successfully modulated its optical properties in aqueous medium. In water, fluorescence quantum yield (η) of **C1** (0.32) was increased up to 0.55 accompanied with 30∼40 nm PL photoluminescence (PL) spectral shifts by forming the self-assembled nanostructure. This vesicular nanostructure may have a potential application as a two-photon molecular tag for biological imaging by two-photon microscopy.*

Keywords Bioimaging; two-photon absorption; two-photon fluorophore; two-photon microscopy

Introduction

During last a few decades, the development of efficient two-photon (TP) materials has attracted considerable interests due to their potentials for optoelectronic and biomedical applications. Two-photon microscopy (TPM) has been used as the best noninvasive bioimaging tool in biological researches and medical diagnosis. It has several advantages including larger penetration depth, reduced photo-damage, better spatial resolution, ability to image turbid samples, and negligible background cellular autofluorescece compared to its single-photon counterpart [1]. However, the lack of suitable water-soluble TP probes has limited the utility of TPM in bioimaging [2]. To develop a useful TP fluorophore, in addition to biocompatibility and photostability, it is crucial to maximize the photoluminescence (PL) quantum efficiency (η) and two-photon absorption (TPA) cross section (δ, expressed in GM $= 1 \times 10^{-50}$ cm^4·photon^{-1}·molecule^{-1}). The quasi linear D-π-A-π-D molecules (where D and A are an electron donor and an acceptor moiety, respectively, and π represents a π-conjugated bridge) with large intramolecular charge transfer (ICT) interaction have shown large δ values [3]. However, η is seriously reduced in a highly polar

*Address correspondence to Han Young Woo, Department of Nano Fusion Technology, Department of Cogno-Mechatronics Engineering (WCU), Pusan National University, Miryang 627-706, Republic of Korea. Fax: +82-55-350-5279; E-mail: hywoo@pusan.ac.kr

aqueous medium due to the ICT-related PL quenching, which actually reduces the product of η and δ (known as two-photon action cross section, $\eta\delta$) and thereby hampers the real imaging performance by reducing the signal to noise ratio. To develop efficient TP probes for TPM has been a challenge.

Here, we have studied the design and optical properties of a cationic TP probe 1,4-bis{4′-[*N*,*N*-bis(6″-trimethylammoniumhexyl)amino]styryl}benzene tetrabromide (**C1**, Scheme 1) by forming a block ionomer complex (BIC) via electrostatic complexation among **C1**, an anionic diblock copolymer, poly[(ethylene oxide)-block-(sodium 2-acrylamido-2-methyl-1-propane sulfonate)] ($\mathbf{E_m}$-$\mathbf{A_n}$, where m = 45, n = 10 or 70) and a cationic surfactant, cetyltrimethylammonium bromide (CTAB). **C1** inside the hydrophobic core of the BIC nanostructure showed a significant increase in fluorescence quantum efficiency accompanied with spectral shifts due to spatial confinement into the hydrophobic microenvironment. In water, fluorescence quantum yield (η) of **C1** (0.32) was increased to 0.41 and 0.55 accompanied with ~30 nm and ~40 nm PL spectral shifts, in the presence of $\mathbf{E_{45}}$-$\mathbf{A_{10}}$/CTAB and $\mathbf{E_{45}}$-$\mathbf{A_{70}}$/CTAB, respectively. This approach may show an important guideline for designing an efficient TP probe for TPM biological imaging.

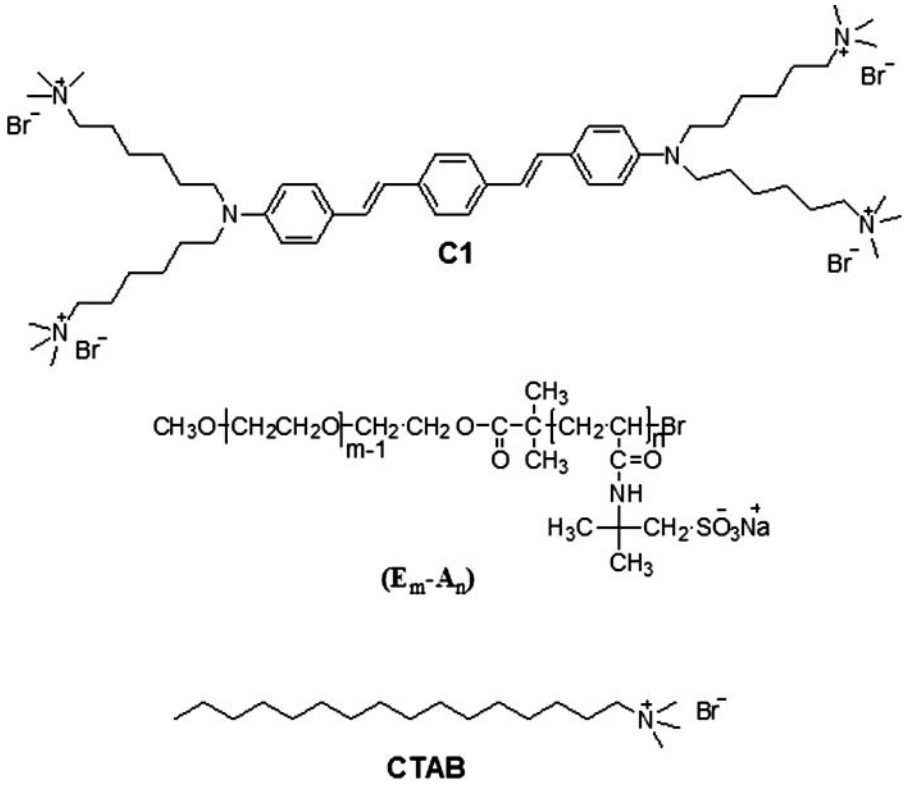

Scheme 1. Chemical structures.

Experiment

All chemicals were purchased from Aldrich Chemical Co., and used as received unless otherwise mentioned. The ^{1}H and ^{13}C NMR spectra were recorded on a JEOL (JNM-AL300) FT NMR system. The UV/vis absorption spectra were measured using a Jasco (V-630)

spectrophotometer. The PL spectra were obtained on a Jasco (FP-6500) spectrofluorometer with a Xenon lamp excitation source, using 90° angle detection for the solution samples. Fluorescence quantum efficiency was measured relative to a freshly prepared aqueous solution of fluorescein at pH ≈ 11 (0.92). Synthesis of the cationic chromophore, **C1** was reported in the previous literature [4]. A series of diblock copolymers, $\mathbf{E_m}$-$\mathbf{A_n}$ having different degree of polymerization (m = 45 and n = 10 or 70) were synthesized by atom transfer radical polymerization (ATRP) by following the published procedures [5]. The block ionomer complexes were prepared as follows: **C1**, ($\mathbf{E_m}$-$\mathbf{A_n}$) and CTAB were separately dissolved in 1 mM phosphate buffer (pH 7.2) solution (PBS). 0.01 mL of 1 mM ($\mathbf{E_m}$-$\mathbf{A_n}$) was added to 2 mL of 5 μM solution of **C1** in a cuvette, and then required amount of 5 mM of CTAB solution was added to the cuvette in portions. For preparation of the BIC complexes, the charge ratio ([−] in ($\mathbf{E_m}$-$\mathbf{A_n}$)/[+] in **C1** and CTAB) was adjusted around 1 at 25 (± 1) °C.

Results and Discussion

A water-soluble cationic two-photon probe **C1**, two anionic diblock copolymers ($\mathbf{E_m}$-$\mathbf{A_n}$) (where m = 45, n = 10 or 70), and a cationic surfactant CTAB were used for preparation of the BIC nanostructure (Scheme 1). The macroinitiator precursor and the diblock copolymers were characterized by ^{1}H NMR and gel filtration chromatography (GFC). Molecular weight distribution of $\mathbf{E_m}$-$\mathbf{A_n}$ was determined by GFC in 0.02 M $NaNO_3$ aqueous solution at 30°C. The number average molecular weight (M_n) of the polymers was determined to be 4,500 g/mol (PDI = 1.29) for $\mathbf{E_{45}}$-$\mathbf{A_{10}}$, 18,000 g/mol (PDI = 1.73) for $\mathbf{E_{45}}$-$\mathbf{A_{70}}$, respectively. **C1** is an ICT-type TP absorbing chromophore with a D-π-A-π-D conjugated backbone and it shows a typical solvatochromism of UV/vis and PL spectra depending on the microenvironment in solution [4, 6]. The absorption and emission maximum wavelengths of **C1** were measured at λ_{abs} = 405 nm and λ_{PL} = 553 nm in PBS (pH 7.2) solution. The PL quantum efficiency was determined to be η = 0.32 for **C1**. When $\mathbf{E_m}$-$\mathbf{A_n}$ ([$\mathbf{E_m}$-$\mathbf{A_n}$] = 5 μM) was added to an aqueous solution of **C1** ([**C1**] = 5 μM in PBS), the absorption and emission intensity substantially decreased with spectral shifts in λ_{abs} and λ_{PL}, which is due to strong aggregation via electrostatic interaction between cationic **C1** and anionic $\mathbf{E_m}$-$\mathbf{A_n}$ (Fig. 1). However, when a cationic surfactant, CTAB was added to the mixture of **C1**

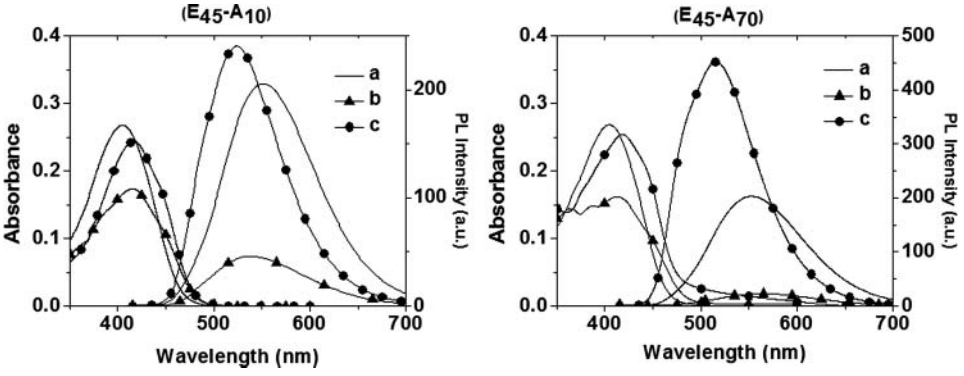

Figure 1. UV/vis and PL spectra of **C1** (a), $\mathbf{C1/E_m}$-$\mathbf{A_n}$ (b), and $\mathbf{C1/E_m}$-$\mathbf{A_n}$/CTAB (c) in PBS. [**C1**] = 5.0 μM, [$\mathbf{E_m}$-$\mathbf{A_n}$] = 5.0 μM, [CTAB] = 40 μM and 325 μM for $\mathbf{C1/E_{45}}$-$\mathbf{A_{10}}$ and $\mathbf{C1/E_{45}}$-$\mathbf{A_{70}}$, respectively. The emission spectra were measured by exciting at λ_{ex} = 405 nm.

Table 1. Optical Properties of C1 in the BIC nanostructures

	C1	C1/E_{45}-A_{10}/CTAB	C1/E_{45}-A_{70}/CTAB
λ_{abs} (nm)[a]	405	419	419
λ_{PL} (nm)[b]	553	524	513
η[c]	0.32	0.41	0.55

[a]Absorption and [b]emission maximum wavelengths, [c]Fluorescence quantum efficiency, ± 10%.

and $\mathbf{E_m}$-$\mathbf{A_n}$, the absorption intensity was recovered with a red-shift in λ_{abs} (405 nm → 419 nm) and the PL intensity also increased accompanied with a blue-shift in λ_{PL} (553 nm → 524∼513 nm), with compared to those of **C1** itself (Table 1). Under this condition, one BIC nanostructure may contain one molecule of **C1** in the core. The spectral changes are most likely due to changes of microenvironment around **C1** by forming a vesicular nanostructure. To get insight into the BIC formation, the PL spectral changes of **C1** was investigated with increasing concentration of CTAB (Fig. 2). It was found that λ_{abs} and λ_{PL} showed a gradual red-shift and blue-shift, with increasing the concentration of CTAB in the mixture. The spectral shift was saturated upon addition of [CTAB] = ∼40 μM for **C1/E_{45}-A_{10}** and ∼325 μM for **C1/E_{45}-A_{70}**. Further addition of CTAB did not lead to any appreciable spectral changes. Here, it should be noted that the concentration (40 μM and 325 μM) of CTAB consumed for the BIC formation of **C1/E_m-A_n**/CTAB is still much lower than its critical micelle concentration (cmc) of CTAB [7]. Thus the process is not a conventional micellization process which is driven by mainly hydrophobic forces and requires the higher concentration than cmc of the surfactant. In all cases, overall charge ratio ([−]/[+]) of anionic $\mathbf{E_m}$-$\mathbf{A_n}$ and cationic (**C1** and CTAB) in the complexes was calculated to be nearly unity at saturation of the spectral changes. This indicates that CTAB interacts with the anionic block of $\mathbf{E_m}$-$\mathbf{A_n}$ by electrostatic interaction. At the spectral saturation, along with the maximum spectral shifts in λ_{abs} and λ_{PL}, the fluorescence quantum efficiency (η) increased from 0.32 (**C1**) to 0.41 for **C1/E_{45}-A_{10}**/CTAB, and 0.55 for **C1/E_{45}-A_{70}**/CTAB, respectively.

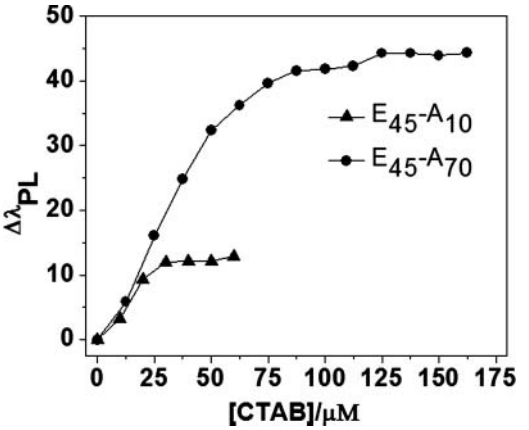

Figure 2. PL spectral changes of **C1** in the presence of $\mathbf{E_m}$-$\mathbf{A_n}$ with increasing [CTAB]. [**C1**] = [$\mathbf{E_m}$-$\mathbf{A_n}$] = 5.0 μM. Where, $\Delta\lambda_{PL} = \lambda_{PL}$(**C1**)—$\lambda_{PL}$(**C1/$E_m$-$A_n$**/CTAB). The PL spectra were measured by exciting at λ_{ex} = 405 nm.

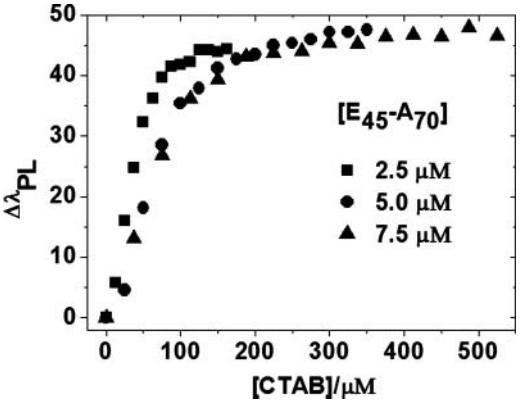

Figure 3. PL spectral changes of **C1** with increasing [CTAB]. [**C1**] = 5.0 μM and [$\mathbf{E_{45}}$-$\mathbf{A_{70}}$] = 2.5, 5.0, and 7.5 μM. $\Delta\lambda_{PL} = \lambda_{PL}$(**C1**)—$\lambda_{PL}$(**C1**/$\mathbf{E_{45}}$-$\mathbf{A_{70}}$/CTAB).

This can be explained in terms of the encapsulation of **C1** inside a non-polar hydrophobic microenvironment by forming the vesicular nanostructure, which induces destabilization of the emitting state (causing a blue-shift in λ_{PL}) of **C1** and reduces the ICT quenching, with enhanced PL efficiency. We also measured the UV/vis and PL spectra of the neutral precursor of **C1**, 1,4-bis{4′-[*N*,*N*-bis(bromohexyl)amino]styryl}benzene (**N1**) in several organic solvents such as n-hexane, toluene, tetrahydrofuran (THF), dichloromethane and dimethyl sufoxide (DMSO). In nonpolar medium such as hexane, **N1** shows the PL emission peaks at 441 nm and 466 nm. With increasing solvent polarity, the emission shows a gradual red-shift with broading of a spectral width. The spectroscopic data are summarized in Table 1. As shown in Fig. 3, we also studied the electrostatic BIC formation of the solution containing [**C1**] = 5.0 μM in the presence of $\mathbf{E_{45}}$-$\mathbf{A_{70}}$ at different concentrations (2.5, 5.0 and 7.5 μM) with changing [CTAB]. In all cases, the complex formation was completed at the charge ratio of [−] in $\mathbf{E_{45}}$-$\mathbf{A_{70}}$/[+] in **C1** and CTAB = ∼1 with saturation of spectral shifts. The 1:1 stoichiometry of [−]/[+] strongly supports that the main driving force of the BIC nanostructure formation is the electrostatic attraction. A set of control experiments were also done under similar conditions using a neutral poly(ethylene oxide) oligomer ($CH_3O(CH_2O)_{45}$-OH) in place of $\mathbf{E_m}$-$\mathbf{A_n}$, which is analogous to the neutral part of the diblock copolymer ($\mathbf{E_m}$-$\mathbf{A_n}$). The measured data show no spectral changes in the PL spectra of **C1** with increasing [CTAB] (Fig. 4). This also confirms that the BIC nanostructure must be formed by electrostatic interaction, which brings **C1** and CTAB molecules in close proximity to $\mathbf{E_m}$-$\mathbf{A_n}$ until charge neutralization, and cooperative binding by hydrophobic forces (as well as electrostatic attraction) among the surfactants tails leads to the formation of a hydrophobic core. Finally the amphiphilic poly(ethylene oxide) block of the copolymer may stabilize the nanostructure by surrounding the neutralized electrostatic complex by hydrophobic interaction, by which the BIC structures still remain to be soluble in water. Previous literatures also support this type of complex formation [8]. In addition, the great advantages of poly(ethylene oxide) enclosed BIC nanostructure are biocompatibility and antifouling property to proteins, blood platelets, and cells [9].

In summary, we have prepared a water-soluble vesicular BIC nanostructure containing a TP probe, 1,4-bis{4′-[*N*,*N*-bis(6″-trimethylammoniumhexyl)amino]styryl}benzene tetrabromide (**C1**) and studied UV/vis and PL spectroscopic properties in water. The microenvironment modulation using the BIC vesicular structure induced ∼2 fold increase in

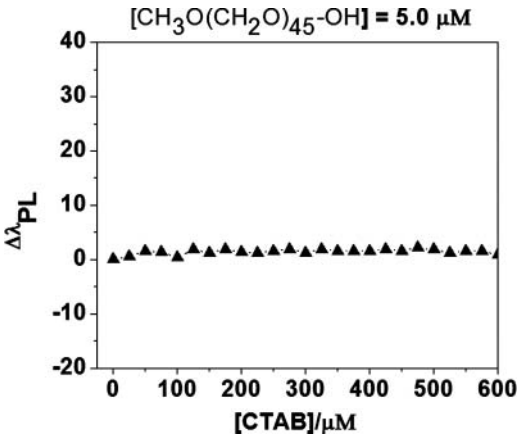

Figure 4. PL spectral changes of **C1** in the presence of $CH_3O(CH_2O)_{45}$-OH with increasing [CTAB]. [**C1**] = 5.0 μM and [$CH_3O(CH_2O)_{45}$-OH] = 5.0 μM. $\Delta\lambda_{PL} = \lambda_{PL}$(**C1**)—$\lambda_{PL}$(**C1**/$CH_3O(CH_2O)_{45}$-OH/CTAB).

the PL quantum efficiency of **C1** with substantial spectral shifts in the BIC complex. This approach may show an important guideline for designing an efficient TP probe for TPM biological imaging in aqueous medium.

Acknowledgements

This work was supported for 2 years by Pusan National University Research Grant.

References

[1] (a) Pawley, J. B. (1995). *Handbook of Biological Confocal Microscopy*, Plenum: New York, 1995. (b) Prasad, P. N. (2003). *Introduction to Biophotonics*, Wiley: NJ. (c) Denk, W., Strickler, J. H., & Webb, W. W. (1990). *Science*, *248*, 73. (d) Helmchen, F., & Denk, W. (2005). *Nat. Methods*, *2*, 932.

[2] (a) Chung, S.-J., Lin, T.-C., Kim, K.-S., He, G. S., Swiatkiewicz, J., Prasad, P. N., Baker, G. A., & Bright, F. V. (2001). *Chem. Mater.*, *13*, 4071. (b) Reinhardt, B. A., Brott, L. L., Clarson S. J., Dillard, A. G., Bhatt, J. C., Kannan, R., Yuan, L., He, G. S., & Prasad, P. N. (1998). *Chem. Mater.*, *10*, 1863.

[3] (a) Zojer, E., Beljonne, D., Kogej, T., Vogel, H., Marder, S. R., Perry, J. W., & Brédas, J.-L. (2002). *J. Chem. Phys.*, *116*, 3646. (b) Albota, M., Beljonne, D., Brédas, J.-L., Ehrlich, J. E., Fu, J.-Y., Heikal, A. A., Hess, S. E., Kogej, T., Levin, M. D., Marder, S. R., McCord-Maughon, D., Perry, J. W., Röckel, H., Rumi, M., Subramaniam, G., Webb, W. W., Wu, X.-L., & Xu, C. (1998). *Science*, *281*, 1653.

[4] Nag, O. K., Nayak, R. R., Lim, C. S., Kim, I. H., Kyhm, K., Cho, B. R., & Woo, H. Y. (2010). *J. Phys. Chem. B*, *114*, 9684.

[5] (a) Robinson, K. L., Weaver, J. V. M., Armes, S. P., Martib, E. D., & Meldrum, F. C. (2002). *J. Mater. Chem.*, *12*, 890. (b) Paneva, D., Mespuille, L., Manolova, N., Degée, P., Rashkov, I., & Dubois, P. (2006). *Macromol. Rapid Commun.*, *27*, 1489.

[6] Woo, H. Y., Korystov, D., Mikhailovsky, A., Nguyen, T., & Bazan, G. C. (2005). *J. Am. Chem. Soc.*, *127*, 13794.

[7] Andeson, M. T., Martin, J. E., Odinek, J. G., & Newcomer, P. P. (1998). *Chem. Mater.*, *10*, 1490.

[8] (a) Wesley, R. D., Dreiss, C. A., Cosgrove, T., Armes, S. P., Thompson, L., Baines, F. L., & Billingham, N. C. (2005). *Langmuir*, *21*, 4856. (b) Kabanov, A. V., Bronich, T. K., Kabanov, V. A., Yu, K., & Eisenberg, A. (1995). *Macromolecules*, *29*, 6797. (c) Liao, X., & Higgins, D. A. (2001). *Langmuir*, *17*, 6051.

[9] (a) Popat, K. C., & Desai, T. A. (2004). *Biosens. Bioelectron.*, *19*, 1037. (b) Malmsten, M., Emoto, K., & Van, A. J. M. (1998). *J. Colloid Interface Sci.*, *202*, 507. (c) Gotoh, Y., Tsukada, M., Minoura, N., & Imai, Y. (1997). *Biomaterials*, *18*, 267. (d) Wang, P., Tan, K. L., Kang, E. T., & Neoh, K. G. (2001). *J. Mater. Chem.*, *11*, 2951. (e) Lopez, G. P., Albers, M. W., Schreiber, S. L., Carroll, R., Peralta, E., & Whitesides, G. M. (1993). *J. Am. Chem. Soc.*, *115*, 5877. (f) Zhang, M., Desai, T., & Ferrari, M. (1998). *Biomaterials*, *19*, 953.